On Dynamics of a Landing Gear Mechanism With Torsional Freeplay

By Elmas Atabay, Ibrahim Ozkol

Istanbul Technical University, Maslak, Istanbul, Turkey

Abstract - In this study, dynamics of a landing gear mechanism with torsional degree of freedom and torsional freeplay is analyzed. Derivation of the equations of motion of the model with torsional degree of freedom and the von Schlippe tire model are presented. Freeplay is introduced into the model and effects of freeplay angles of 0 ^{O}, 0.5^O, 1^O and 1.5^O are observed by obtaining time histories of the torsion angle and lateral tire deformation and limit cycles of the torsionangle. Amplitudes and frequencies of oscillations of the time histories of the torsion angle and lateral tire deformation are presented.

ON DYNAMICS OF A LANDING GEAR MECHANISMWITH TORSIONAL FREEPLAY

Strictly as per the compliance and regulations of:

On Dynamics of a Landing Gear Mechanism With Torsional Freeplay

Elmas Atabay[α], Ibrahim Ozkol[σ]

Abstract - In this study, dynamics of a landing gear mechanism with torsional degree of freedom and torsional freeplay is analyzed. Derivation of the equations of motion of the model with torsional degree of freedom and the von Schlippe tire model are presented. Freeplay is introduced into the model and effects of freeplay angles of 0 °, 0.5º, 1º and 1.5º are observed by obtaining time histories of the torsion angle and lateral tire deformation and limit cycles of the torsion angle. Amplitudes and frequencies of oscillations of the time histories of the torsion angle and lateral tire deformation are presented.

I. Introduction

Vibration of aircraft steering systems has been a problem of great concern since the production of first airplanes. Shimmy is an oscillatory motion of the landing gear in lateral and torsional directions, caused by the interaction between the dynamics of the tire and the landing gear, with a frequency range of 10–30 Hz. Though it can occur in both nose and main landing gear, the first one is more common. Shimmy is a dangerous condition of selfexcited oscillations driven by the interaction between the tires and the ground that can occur in any wheeled vehicle. Problem of shimmy occurs in ground vehicle dynamics and aircraft during taxiing and landing. In other words, shimmy takes places either during landing, take–off or taxi and is driven by the kinetic energy of the forward motion of the aircraft. It is a combined motion of the wheel in lateral, torsional and longitudinal directions.

II. Shimmy

Shimmy can occur in steerable wheels of cars, trucks and motorcycles, as well as trailers and tea carts. In vehicle dynamics, shimmy is the unwanted oscillation of a rolling wheel about a vertical axis. It can occur in taxiing aircraft, as well. In the case of a shopping cart wheel, it is caused by the coupling between transverse and pivot degrees of freedom of the wheel. In the case of landing gear, shimmy is the result of the coupling between tire forces and landing gear bending and torsion. In other words, basic cause of shimmy is energy transfer from tireground contact force and vibration modes of the landing gear system.

Shimmy is an unstable phenomenon and it occurring with a certain combination of parameters such as mass, elastic quantities, damping, geometrical quantities, speed, excitation forces and nonlinearities such as friction and freeplay. It is difficult to determine shimmy analytically since it is a very complex phenomenon, due to factors such as wear and ground conditions that are hard to model. Small differences in physical conditions can lead to extremely different results. For example, it is reported in [1] that a new small fighter aircraft whose name is withheld, has displayed to vibrations during low and high speed taxi tests and first several landings and takeoffs, but shimmy vibrations with frequencies in the range 22–26 Hz were experienced during next several landings and take–offs at certain speeds, especially during landing. This demonstrates the effect of wear on landing gear shimmy. In the reported case, it was seen that tightening the rack too tight against the pinion prevented the wheel from turning, while tightening it less tight caused the vibration to disappear but reappear in the following flights.

Ground control of aircraft is extremely important since severe shimmy can result in loss of control or fatigue failure of landing gear components. Vibration of aircraft steering systems deserves and has gained attention since shimmy is one of the most important problems in landing gear design. Shimmy is reported to be due to the forces produced by runway surface irregularities and nonuniformities of the wheels [2–5]. Modeling of aircraft tires presents similar challenges to those involved in modeling automotive tires in ground vehicle dynamics, on a much larger scale in terms size and loads on the tire [6].

Shimmy is a complex phenomenon influenced by many parameters. Causes of shimmy can be listed as follows [2,7–10].

- Insufficient overall torsional stiffness of the gear about the swivel axis
- Inadequate trail, since positive trail reduces shimmy
- Improper wheel mass balancing about the swivel axis
- Excessive torsional freeplay
- Low torsional stiffness of the strut
- Flexibilities in the design of the suspension
- Surface irregularities
- Nonuniformities of the wheels
- Worn parts

Author [α],[σ] : Istanbul Technical University, Department of Aeronautical Engineering, Maslak, Istanbul, Turkey.
E-mail : anli@itu.edu.tr, ozkol@itu.edu.tr

III. Detection and Suppression of Shimmy

Shimmy is a great concern in aircraft landing gear design and maintenance. Prediction of nose landing gear shimmy is an essential step in landing gear design because shimmy oscillations are often detected during the taxi or runway tests of an aircraft, when it is no longer feasible to make changes on the geometry or stiffness of the landing gear. Although shimmy was observed in earlier aircraft as well, there were no extra shimmy damping equipments installed. Historically, France and Germany tended to deal with shimmy in the design phase, while in United States, the trend was to solve the problem after its occurrence. Currently, the general methodology is to employ a shimmy damper and structural damping. A shimmy damper, acting like a shock absorber in a rotary manner, is often installed in the steering degree of freedom to damp shimmy. It is a hydraulic damper with stroke limited to a few degrees of yaw. A shimmy damper restrains the movement of the nose wheel, allowing the wheel to be steered by moving it slowly, but not allowing it to move back and forth rapidly. It consists of a tube filled with hydraulic fluid causing velocity dependent viscous damping forces to form when a shaft and piston are moved through the fluid. Oleo–pneumatic shock absorbers are the most common shock absorber system in medium to large aircraft, since they provide the best shock absorption ability and effective damping. Such an absorber has two components: a chamber filled with compressed gas, acting as a spring and absorbing the vertical shock and hydraulic fluid forced through a small orifice, forming friction, slowing the oil and causing damping. Another common cure is to replace the tires even though they may not be worn out [10–12].

Shimmy started being investigated in 1920's both theoretically and experimentally and soon it became clear that it is caused not by a single parameter but by the relationships between parameters. Effects of acceleration and deceleration on shimmy have been reported to be examined, and the accelerating system is found to be slightly less stable [13]. Number of publications available in literature on landing gear shimmy is limited because many developments are proprietary and are not published in literature.

IV. Literature Survey

Many papers have been published addressing shimmy as a vehicle dynamics problem. In that perspective, tire is the most important item, and tire models have been investigated. [13] examines the wheel shimmy problem and its relationship with longitudinal tire forces, vehicle motions and normal load oscillations. [8] compares different dynamic tire models for the analysis of shimmy instability. [3] is an investigation of tire parameter variations in wheel shimmy, by considering the shimmy resulting from the elasticity of a pneumatic tire, particularly in taxiing aircraft. [14] is on the application of perturbation methods to investigate the limit cycle amplitude and stability of the wheel shimmy problem. [7] deals with the shimmy stability of twin–wheeled cantilevered aircraft main landing gear. The objective in [15] is to develop software on assessing shimmy stability of a general class of landing gear designs using linear and nonlinear landing gear shimmy models. [16] studies the periodic shimmy vibrations and chaotic vibrations of a simplified wheel model using bifurcation theory. [17] is on tire dynamics and is a development to deal with large camber angles and inflation pressure changes. [18] is another study on tire dynamics, where stability charts show the behavior of the system in terms of certain parameters such as speed, caster length, damping coefficient and relaxation length. [19] is an experimental study on wheel shimmy where system parameters are identified, stability boundaries and vibration frequencies are obtained on a test rig for an elastic tire. Dependence of shimmy oscillations in the nose landing gear of an aircraft on tire inflation pressure are investigated in [20]. The model derived in [21] is used and it is concluded that landing gear is less susceptible to shimmy oscillations at inflation pressures higher than the nominal.

Transverse vibrations of landing gear struts with respect to a hull of infinite mass have been studied theoretically in [22]. Similarly, [23] presents a nonlinear model describing the dynamics of the main gear wheels relative to the fuselage.

Lateral dynamics of nose landing gear shimmy models has gained some attention. Lateral response of a nose landing gear has been investigated in [10] where nonlinearities arise due to torsional freeplay. In [24], lateral response to ground–induced excitations due to runway roughness is taken into consideration as well. Lateral stability of a nose landing gear with a closed loop hydraulic shimmy damper is presented in [12]. Closed form analytical expressions for shimmy velocity and shimmy frequency are derived in regard to the lateral dynamics of a nose landing gear in [25].

A dynamic model of an aircraft nosegear is developed in [9] and effects of design parameters such as energy absorption coefficient of the shimmy damper, the location of the center of gravity of the landing gear, shock strut elasticity, tire compliance, friction between the tire and the runway surface and the forward speed on shimmy are investigated. It is shown in [26] that dry friction is one of the principal causes of shimmy.

Bifurcation analysis of a nosegear with torsional and lateral degrees of freedom is performed in [21]. Similarly, bifurcation analysis of a nosegear with torsional, lateral and longitudinal modes is performed in [27]. In a more mathematical study, incremental harmonic balance method is applied to an aircraft wheel shimmy system with Coulomb and quadratic damping [28] and amplitudes of limit cycles are predicted.

Theoretical research on shimmy has a long history, with the initial focus on tire dynamic behavior because tires play an important role in causing shimmy instability. Theories on tire models can be divided into stretched string models and point contact models. In the stretched string model proposed by von Schlippe, the tire centerline is represented as a string in tension, the tire sidewalls are represented by a distributed spring where the string rests and the wheel is represented by a rigid foundation for the spring. Pacejka has proposed replacing the string by a beam. The point contact method assumes the effects of the ground on the tire act at a single contact point and is much easier to implement in an analytical model.

V. MATHEMATICAL MODE

a) Landing gear model

In this study, dynamics of a landing gear model with torsional degree of freedom and torsional freeplay is analyzed. The nonlinear mathematical shimmy model presented in [11], [29] and [30] describes the torsional dynamics of the lower parts of a landing gear mechanism and stretched string tire model. Figures 1 a and b show the physical and mathematical nose landing gear models. Dynamics of the lower part of the landing gear is described by a second order ordinary differential equation for the yaw angle y about the vertical axis z, while the dynamics of the tire modeled with respect to the stretched string tire model is described by a first order ordinary differential equation for the lateral tire deflection y.
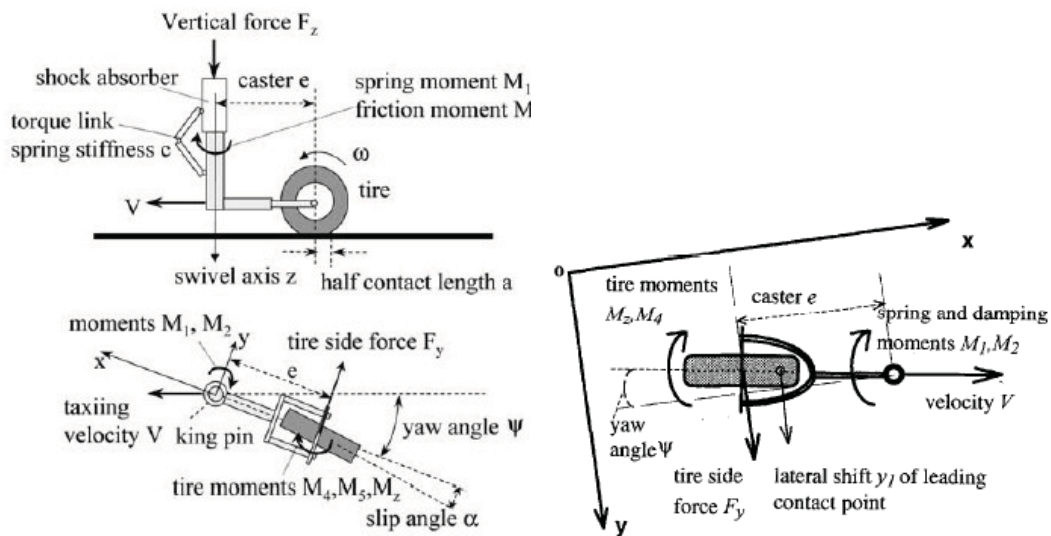

Figure 1: a. Nose landing gear model [30], b. shimmy dynamics model [29].

$$I_z \ddot{\psi} = M_1 + M_2 + M_3 + M_4 \qquad (1)$$

where I_z is the moment of inertia about the z axis,

M_1 is the linear spring moment between the turning tube and the torque link,

M_2 is the combined damping moment from viscous friction in the bearings of the oleo–pneumatic shock absorber and from the shimmy damper,

M_3 is the tire moment about the z axis and

M_4 is the tire damping moment due to tire tread width..

M_1 and M_4 are external moments.

M_3 and M_4 are caused by lateral tire deformations due to side slip.

M_3 is composed of M_z, tire aligning moment about the tire center, and tire cornering moment eF_y. F_y is the wheel cornering force or the sideslip force acting with caster e as lever arm.

$$M_1 = k \dot{\psi} \qquad (2)$$

$$M_2 = c \psi \qquad (3)$$

$$M_3 = M_z - e F_y \qquad (4)$$

$$M_4 = \frac{\kappa}{v} \dot{\psi} \qquad (5)$$

where k is the torsional spring rate, c is the torsional damping constant, v is the taxiing velocity and k is the tread width moment constant defined as [29]

$$\kappa = -0.15\, a^2 c_{F\alpha}\, F_z \qquad (6)$$

F_y and M_z depend on the vertical force F_z and slip angle . Tire sideslip characteristics are nonlinear. Cornering force F_y and vertical force F_z are related as

$$F_y/F_z = c_{F\alpha}\alpha, \qquad \text{for } |\alpha| \le \delta \qquad (7)$$

$$F_y/F_z = c_{F\alpha}\delta\, sign(\alpha), \quad \text{for } |\alpha| > \delta \qquad (8)$$

Where δ is the limiting slip angle or the limit angle of tire force and $sign(\alpha)$ is the sign function defined as

$$sign(\alpha) = \begin{cases} 1, \text{if } \alpha > \delta \\ -1, \text{if } \alpha \le \delta \end{cases} \qquad (9)$$

Slip angle may be caused by either pure yaw or pure sideslip. Pure yaw occurs when the yaw angle ψ is allowed to vary while the lateral deflection y is held at zero. Pure sideslip, on the other hand, occurs when the lateral deflection y is allowed to vary as the yaw angle ψ is held at zero [11].

An expression is given for the nonlinear sideslip characteristic in the widely used Magic Formula [7, 11, 17] as the following

$$F_y = D \sin\,[C \arctan\{B\alpha - E\,(B\alpha - \arctan(B\,\alpha))\}] \quad (10)$$

where B,C, D and E are functions of the wheel load, slip angle, slip ratio and camber. B and E are related to vertical force F_z, C is the shape factor and D is the peak value of the curve.

Plots of F_y/F_z versus α will not be presented here due to lack of space, but they have similar characteristics when obtained using either (7) and (8) or the Magic Formula, thus the simple approximations given by (7) and (8) are used instead of the complicated Magic Formula. Only force and moment derivatives are needed as parameters for (7) and (8).

Aligning moment M_z is defined using a half–period sine. M_z/F_z is approximated by a sinusoidal function and the constant zero given by (11) and (12).

$$M_z/F_z = c_{M\alpha}\frac{\alpha_g}{180}\sin\left(\frac{180}{\alpha_g}\alpha\right), \quad \text{for } |\alpha| \le \alpha_g \ (11)$$

$$M_z/F_z = 0, \qquad \text{for } |\alpha| > \alpha_g \ (12)$$

where α_g is the limiting angle of tire moment.

b) Tire model

Tire is modeled using the elastic string theory. Lateral deflection of the tire is described as [11,29]

$$\dot{y} + \frac{v}{\sigma}y = v\psi + (e - a)\dot{\psi} \qquad (13)$$

Ground forces are transmitted to the wheel through the tire, and these forces acting on the tire footprint deflect the tire. Elastic string theory states that lateral deflection y of the leading contact point of the tire with respect to tire plane can be described as a first order differential equation given by (13). This equation is derived as follows.

Tire sideslip velocity V_t is expressed as

$$V_t = \dot{y} + \frac{y}{\tau} \qquad (14)$$

Where $\tau = \dfrac{\sigma}{V}$ is the time constant, σ is the relaxation length, which is the ratio of the slip stiffness to longitudinal force stiffness. The tire also undergoes yaw motion, leading to a yaw velocity V_r which is approximated as

$$V_r = v\psi + (e - a)\dot{\psi} \qquad (15)$$

As the wheel rolls on the ground,

$$V_t = V_r \qquad (16)$$

Substituting (14) and (15) into (16) yields (13).

An equivalent side slip angle caused by lateral deflection is used to compute cornering force F_y and aligning moment M_z and is approximated as

$$\alpha \approx \arctan\alpha = \frac{y}{\sigma} \qquad (17)$$

Equations (1), (13) and (17) constitute the governing equations of the torsional motion of the landing gear and include nonlinear tire force and moment. Parameters of a light aircraft used in the computations are given in table 1.

Table 1: Parameters used in the torsional dynamics.

Parameter	Description	Value	Unit
v	velocity	0…80	m/s
a	half contact length	0.1	m
e	caster length	0.1	m
I_z	moment of inertia	1	kg m^2
F_z	vertical force	9000	N
c	torsional spring rate	-100000	Nm/rad
$c_{F\alpha}$	side force derivative	20	1/rad
$c_{M\alpha}$	moment derivative	-2	m/rad
k	torsional damping constant	0…-50	Nm/rad/s
κ	tread width moment constant	-270	Nm^2/rad
$\sigma = 3a$	relaxation length	0.3	m
α_g	limit angle of tire moment	10	deg
δ	limit angle of tire force	5	deg

c) Linearization

In order to use linear analysis tools, nonlinear landing gear model has to be linearized. Following this, linear stability analysis will be performed.

within a small range of the side slip angle α, cornering force F_y and the ratio $M_z \, / \, F_z$ can be approximated proportional to the side slip angle. Based on this assumption, substituting equations (7), (8), (11) and (12) into (4) yields (20), the complete expression for the tire moment M_3

$$F_y = \begin{cases} c_{F\alpha}\alpha F_z, & |\alpha| \le \delta \\ c_{F\alpha}\delta \, sign(\alpha), & |\alpha| > \delta \end{cases} \tag{18}$$

$$M_z = \begin{cases} c_{M\alpha}\dfrac{\alpha_g}{180}\sin\left(\dfrac{180}{\alpha_g}\alpha\right)F_z, & |\alpha| \le \alpha_g \\ 0, & |\alpha| \ge \alpha_g \end{cases} \tag{19}$$

$$M_3 = \begin{cases} -ec_{F\alpha}\delta \, sign(\alpha)\,F_z, & \alpha \le -\alpha_g \\ c_{M\alpha}\dfrac{\alpha_g}{180}\sin\left(\dfrac{180}{\alpha_g}\alpha\right)F_z - ec_{F\alpha}\delta \, sign(\alpha)\,F_z, & -\alpha_g < \alpha < -\delta \\ c_{M\alpha}\dfrac{\alpha_g}{180}\sin\left(\dfrac{180}{\alpha_g}\alpha\right)F_z - ec_{F\alpha}\delta \, F_z, & -\delta < \alpha < \delta \\ c_{M\alpha}\dfrac{\alpha_g}{180}\sin\left(\dfrac{180}{\alpha_g}\alpha\right)F_z - ec_{F\alpha}\delta \, sign(\alpha)\,F_z, & \delta < \alpha < \alpha_g \\ ec_{F\alpha}\delta \, sign(\alpha)\,F_z, & \alpha > \alpha_g \end{cases} \tag{20}$$

Substituting (17) into (20) and expressing M_3 in the neighborhood of a = 0 or y = 0 yields

$$M_3 = c_{M\alpha}\frac{\alpha_g}{180}\sin\left(\frac{180}{\alpha_g}\frac{y}{\sigma}\right)F_z - ec_{F\alpha}\frac{y}{\sigma}F_z \tag{21}$$

M_3 can be linearized using the Taylor series expansion as

$$\left.\frac{\partial M_3}{\partial y}\right|_{y=0} = c_{M\alpha}\frac{\alpha_g}{180}\cos\left(\frac{180}{\alpha_g}\frac{y}{\sigma}\right)F_z\frac{180}{\alpha_g\sigma} - ec_{F\alpha}\frac{1}{\sigma}F_z\bigg|_{y=0} = \frac{F_z}{\sigma}\left(c_{M\alpha} - ec_{F\alpha}\right) \tag{22}$$

Defining the state variables as $(\psi, \dot\psi, y)$ gives the linearized model as three ordinary differential equations of first order as

$$\begin{bmatrix} \dot\psi \\ \ddot\psi \\ \dot y \end{bmatrix} = \begin{bmatrix} 0 & 1 & 0 \\ c_1 & c_2 & c_3 \\ v & c_4 & c_5 \end{bmatrix} \begin{bmatrix} \psi \\ \dot\psi \\ y \end{bmatrix} \tag{23}$$

where

$$c_1 = \frac{c}{I_z} \tag{24}$$

$$c_2 = \frac{k}{I_z} + \frac{\kappa}{vI_z} \tag{25}$$

$$c_3 = \frac{\left(c_{M\alpha} - ec_{F\alpha}\right)F_z}{I_z\sigma} \tag{26}$$

$$c_4 = e - a \tag{27}$$

$$c_5 = \frac{-v}{\sigma} \tag{28}$$

VI. Freeplay

Freeplay is a type of concentrated structural nonlinearity inherent in many mechanical systems. Such concentrated structural nonlinearities, such as cubic, freeplay and hysteresis stiffnesses, have significant effects on aeroelastic responses of airfoil surfaces. Freeplay gives the most critical flutter condition among the three and is inevitable for control surfaces due to wear and manufacturing errors. It exists in the hinge part of the control surfaces of most flight vehicles and is generated from loose or worn hinge connections, joint slippage and manufacturing tolerances. Freeplay may couple with aerodynamic effects and cause limit cycle oscillations during flight, leading to structural damage due to fatigue. Thus, it is crucial to incorporate freeplay into the equations of motion and to predict its effects in advance. Freeplay nonlinearity causes structural stiffness to become piecewise continuous. A spring is often used in literature to represent worn or loose control surface hinges. Most of the literature considering the effect of freeplay concentrates on problems of aeroelasticity. Missile control surfaces, moveable aircraft lifting surfaces such as horizontal tails or rotatable pylons on aircraft with variable sweep exhibit freeplay that can be potentially dangerous from an aeroelastic perspective, in terms of flutter conditions. It is found that limit cycle oscillations in the case of freeplay nonlinearity occur below the linear flutter speed boundary, which means the critical flutter speed is below that of the system without freeplay. Additionally, freeplay may cause instabilities both above and below the flutter speed predicted by the linear theory. Responses to freeplay include nonlinear phenomena such as limit cycle oscillations and even chaotic responses. Limit cycle oscillations are likely to occur in the presence of freeplay nonlinearities, leading to fatigue and damage in the long run. The possibility of even small freeplay angles leading to severe instabilities dangerous fatigue conditions are shown in literature [31–34,35,36,37].

Cyclic loading occurs during taxi due to runway surface irregularities, which may lead to wear in mechanical components of the landing gear, including freeplay in the rack and pinion of the steering system, interlinkages of the torque link, fuselage attachment points, steering collar and wheel axle [38].

Freeplay is hard to avoid in loose or old joints. Its existence may affect the system response, even leading to chaos, however harmful results can be avoided if possible limit cycle oscillations or chaotic motion are known in advance. Therefore, it is important to determine the possibility of the existence of such motions before they occur [31–33]. Additionally, freeplay will have an effect on the response of the system to a control law that was initially designed for the linear model [39]. Although freeplay is often linearized or ignored in calculations, it is necessary to compare the responses of the systems with and without freeplay. Amount of freeplay present in the studies mentioned here are in the range 0.1º–2.12º.

Various parts of the landing gear move with respect to each other during landing impact and when retracted. Freeplay at the wheel axle due to the contributions from various connections are less then one degree in yaw and in the order of millimeters in the lateral and fore/aft directions. It has been verified experimentally that the amount of freeplay is a function of the shock absorber deflection. Free play will increase with the number of flights. Application of tight tolerances might help in solving shimmy problems in the prototype phase, however, the problem will reoccur when the aircraft is in service, due to wear [7].

VII. Literature Survey On Freeplay

A literature survey on freeplay reveals that freeplay has been considered mostly by researchers working on the fluid–structure interaction problem. Flutter analysis of airfoils with freeplay nonlinearities in pitch degree of freedom subject to incompressible flow have gained some attention. Limit cycle oscillations of airfoils having two degrees of freedom and freeplay nonlinearities in pitch, placed in transonic and supersonic flows are investigated in [31] and [32], respectively. Similar numerical studies investigating the same model are [40], where the model is placed in subsonic and transonic flows, [37], where the model is placed in transonic and low supersonic flows, and [41], where the model is placed in turbulent flow. Bifurcation analysis of the same system with two degrees of freedom is conducted in [42].

Mathematical analysis of the behavior of a two dimensional aeroelastic system with freeplay nonlinearity is presented in [43] and two formulations are developed. Formulations are extended for a hysteresis model in [44]. Unlike a freeplay model which consists of three linear subsystems, a hysteresis model consists of six.

Bifurcation analysis an airfoil having two degrees of freedom with both freeplay and cubic stiffness nonlinearities in pitch placed in supersonic flow has been conducted in [35]. Bifurcation analysis of an aircraft with freeplay nonlinearity is conducted in [45]. Limit cycle oscillations of an airfoil with two degrees of freedo having freeplay in the pitching degree of freedom are examined experimentally and theoretically in [34]. An experimental delta wing model with freeplay at the attachment points is designed and tested in [46], and its gust response is investigated in [47]. Effect of freeplay on the aerodynamic response, such as limit cycle flutter, has been examined. It has been found that the amplitude and position of the limit cycle varies with the magnitude of freeplay. Effects of variations in parameters have been examined for both the damped and limit cycle oscillations. Critical flutter speeds are predicted.

Hinges of control surfaces often demonstrate freeplay nonlinearity. [48] is a study examining the limit cycle oscillations of a combination of an airfoil and an aileron, resulting in three degrees of freedom, with freeplay in the aileron hinge. Aeroelastic response of other two dimensional systems having control surface freeplay nonlinearity are studied using the harmonic balance approach in [49] and both numerically and experimentally in [39]. A dissertation was presented to Duke University in 2000, covering the dynamics of a two dimensional aeroelastic system with control surface freeplay nonlinearity, both experimentally and mathematically [50]. Limit cycle oscillations are observed. The system is very similar to the one given in [48], a combination of an airfoil with an aileron.

A three dimensional control surface with play is investigated in [51] to demonstrate the effects of angle of attack and Mach number. Flutter analysis of a missile wing having freeplay in it the rotation degree of freedom of the wing control mechanism is conducted in [33] by investigating limit cycles and chaotic motion. Results state that the system response depends on the amount of freeplay and initial conditions.

A study on a mechanical system exhibiting freeplay nonlinearity is studied both numerically and experimentally in [36] where the problem of developing a mathematical model and performing a simulation of the dynamics of systems exhibiting freeplay nonlinearity is addressed. Contact due to freeplay is considered, constraints are formulized and the stability of an aircraft wing displaying freeplay in the hinge supporting a control surface is investigated. Freeplay is considered as one of the rotor faults in the simulation of helicopter structural damages in [52].

Freeplay model used in this study is based on the ones in [31] and [38]. Dynamics of a landing gear mechanism with freeplay in the torsional degree of freedom is analyzed in [38], while dynamic behavior of a two dimensional airfoil with freeplay in pitch, oscillating in pitch and plunge directions, subjected to inviscid, transonic flow is analyzed in [31]. Both freeplay nonlinearities are modeled using the same principle and formulation, although the two studies are in two very distinct disciplines. Same formulation as in [31] is employed in [40,93], and mathematical models given in [32,33,35,37,41–43,48] are also similar .

Freeplay is modeled as a nonlinear spring as in figure 2, where some deflection is possible before a force develops and the spring force is zero if the amplitude remains within the freeplay band. Formulations have been suggested in literature to determine an equivalent linear stiffness.
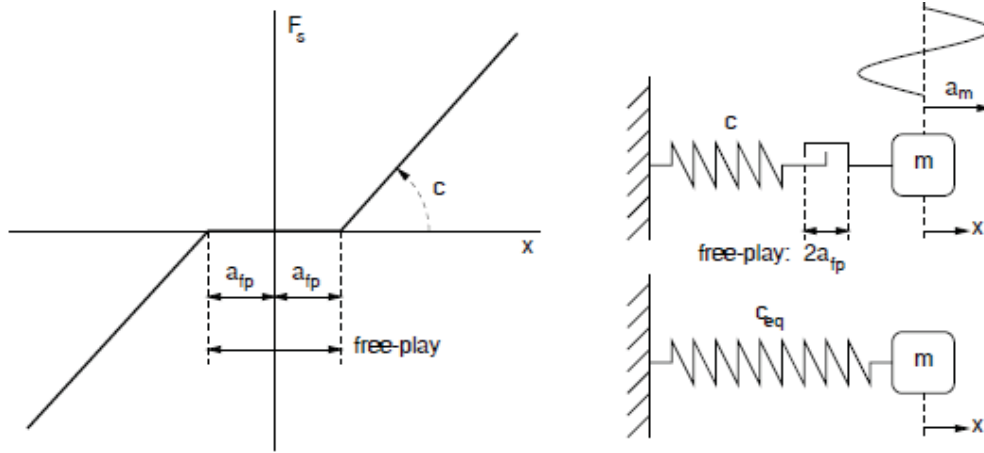
Figure 2 : Modeling of freeplay [7].

Equation 34 gives the piecewise continuous restoring moment function similar to the one used in [38] to describe the concentrated nonlinearity at the torsional degree of freedom.

$$M(\psi) = \begin{cases} K_\psi(\psi - \psi_{fp}) & \text{if } \psi \geq \psi_{fp} \\ 0 & \text{if } -\psi_{fp} \leq \psi \leq \psi_{fp} \\ K_\psi(\psi + \psi_{fp}) & \text{if } \psi \leq -\psi_{fp} \end{cases} \tag{29}$$

Torsion is denoted by ψ, K_ψ is the stiffness coefficientand ψ_{fp} is the freeplay angle.

VIII. Incorporation of Freeplay into the Landing Gear Model

Torsional freeplay is incorporated into the equations of motion of the landing gear. Results are displayed for various values of the freeplay angle ψ_{fp} within the range 0°–2°, as this is the range employed in literature. Freeplay has been incorporated into the equations of motion of landing gear mechanisms in very few studies literature [38].

Freeplay model given in (29) can be incorporated in the equations of motion in two ways. One of them, is to linearize the model as in (23)–(28) and substitute (29) into $c_1\psi$ in (23). This way, the only nonlinearity in the model is freeplay nonlinearity such that the second equation in (23) becomes

$$\ddot{\psi} = M(\psi) + c_2\dot{\psi} + c_3 y \tag{30}$$

Second way of incorporating freeplay nonlinearity in the model is to obtain a more realistic model by substituting (29) directly into the nonlinear model. This is the approach taken here. Nonlinear equations are integrated using the fourth order Runge–Kutta algorithm.

IX. Results

Effects of freeplay are observed by obtaining time histories of the torsion angle and lateral tire deformation and limit cycles. Freeplay angles of 0°, 0.5°, 1° and 1.5° are incorporated. Amplitudes and frequencies of oscillations of the time histories of the torsion angle and lateral tire deformation are presented in tables 2 and 3, respectively.

a) Effect of freeplay on the torsion angle

Time histories of the torsion angle are presented for freeplay angles of 0°, 0.5°, 1° and 1.5° in figures 3–6 for $\psi(0) = 0.1$. Amplitudes and frequencies of oscillations of the time histories of the torsion angle are presented in table 2.
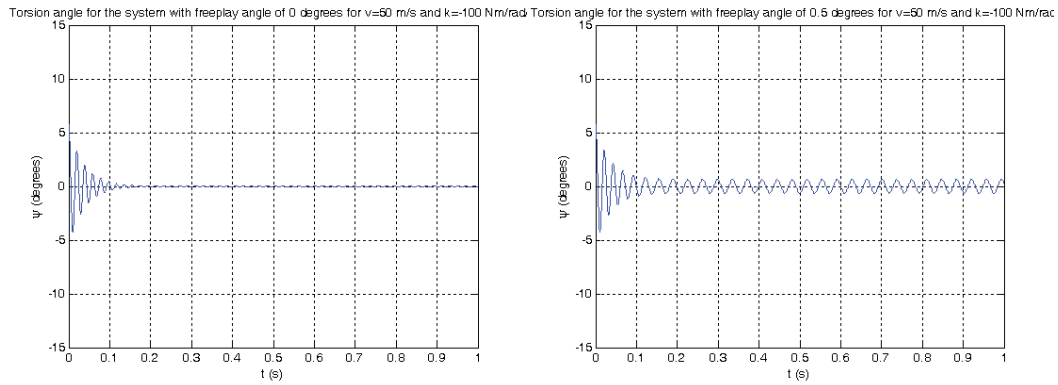
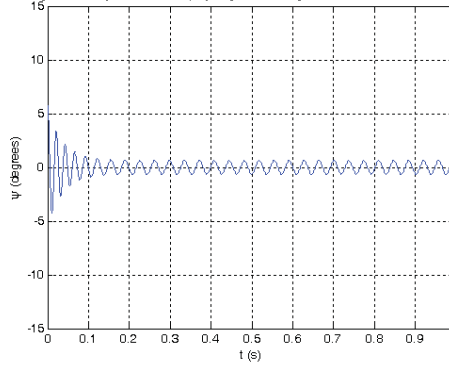Figure 3 : Torsion angle for ψ_{fp} of 0º.
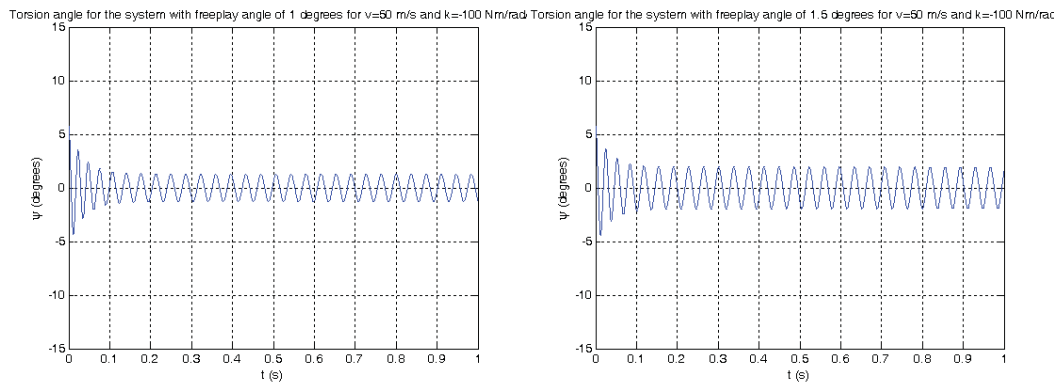

Figure 4 : Torsion angle for ψ_{fp} of 0.5º.
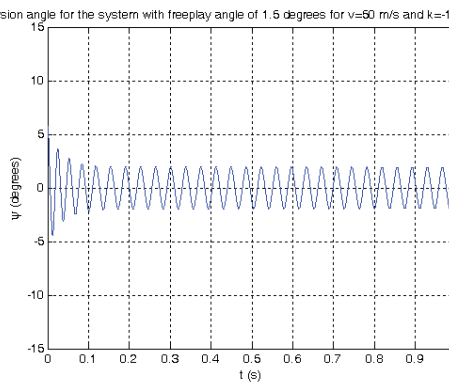

Figure 5 : Torsion angle ψ_{fp} of 1º.

Figure 6 : Torsion angle for ψ_{fp} of 1.5º.

Table 2 : Amplitudes and frequencies of the torsion angle for various

ψ_{fp}	amplitude	frequency
0º	oscillation decays after 0.2 s	-
0.5º	1º	29 Hz
1º	2º	28 Hz
1.5º	2.5º	27 Hz

b)   Effect of freeplay on the lateral tire deformation

Time histories of the lateral tire deformation are presented for freeplay angles of 0º, 0.5º, 1º and 1.5º in figures 7–10 for $\psi(0) = 0.01$ and in figures 11–14 for $\psi(0) = 0.1$. Amplitudes and frequencies of oscillations of the time histories of the lateral tire deformation are presented in table 3 for $\psi(0) = 0.01$ and in table 4 for $\psi(0) = 0.1$.
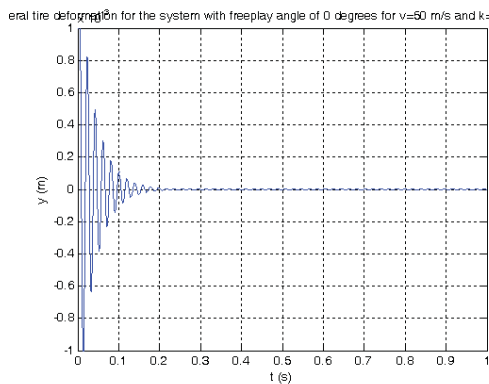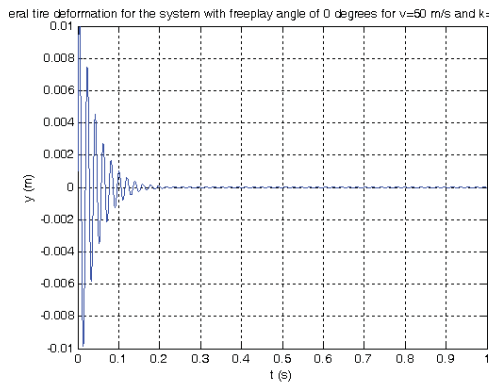

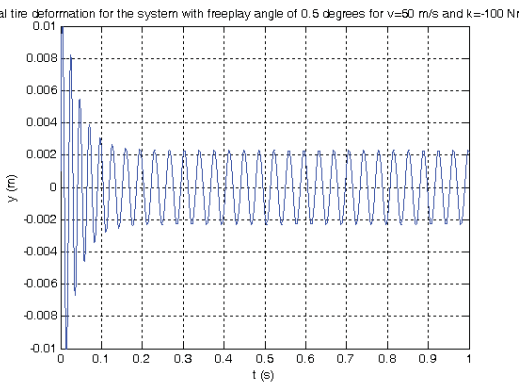Figure 7 : Lateral tire deformation for ψ_{fp} of 0º.
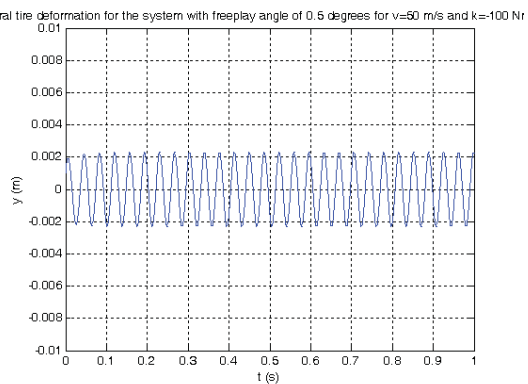
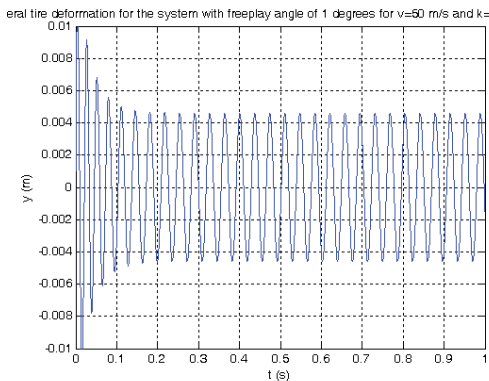Figure 8 : Lateral tire deformation for ψ_{fp} of 0.5º.
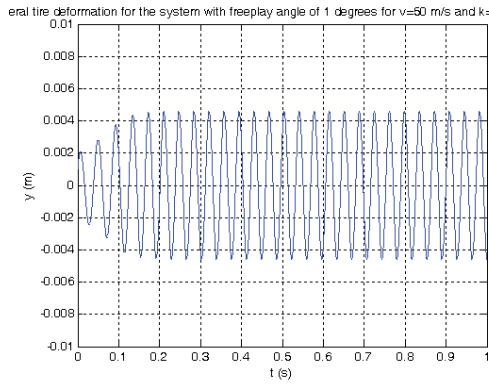
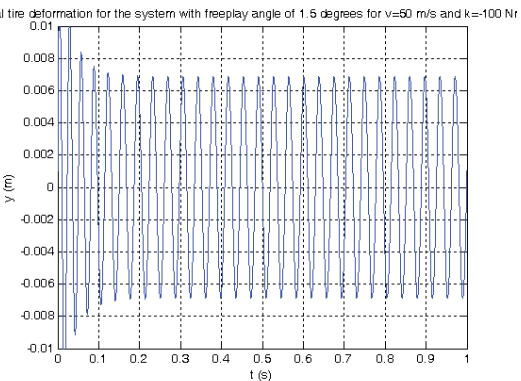*Figure 9 :* Lateral tire deformation for ψ_{fp} of 1º.   *Figure10 :* Lateral tire deformation for ψ_{fp} of 1.5º.
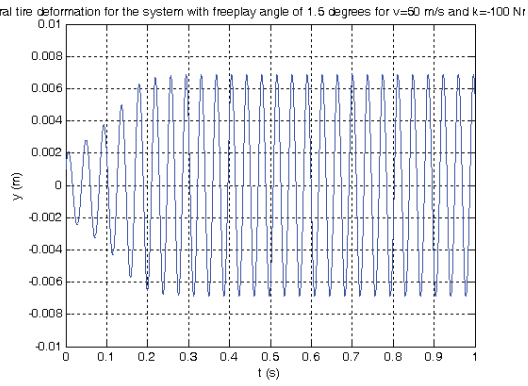
Table 3 : Amplitudes and frequencies of the lateral tire deformation for various ψ_{fp} and $\psi(0) = 0.01$.

ψ_{fp}	amplitude	frequency
0º	oscillation decays after 0.2 s	-
0.5º	$2 * 10^{-3}$ m	27 Hz
1º	$4.5 * 10^{-3}$ m	26 Hz
1.5º	$7 * 10^{-3}$ m	26 Hz

Figure11: Lateral tire deformation for ψ_{fp} of 0º.   *Figure 12 :* Lateral tire deformation for ψ_{fp} of 0.5º.

Figure13 : Lateral tire deformation for ψ_{fp} of 1º.   *Figure14 :* Lateral tire deformation for ψ_{fp} of 1.5º.

Table 4 : Amplitudes and frequencies of the lateral tire deformation for various ψ_{fp} and $\psi(0)=0.1$.

ψ_{fp}	amplitude	frequency
0°	oscillation decays after 0.2 s	-
0.5°	$2.2 * 10^{-3}$ m	29 Hz
1°	$4.5 * 10^{-3}$ m	28 Hz
1.5°	$7 * 10^{-3}$ m	28 Hz

c) Effect of freeplay on limit cycles

Limit cycles of the torsion angle are obtained for $\psi(0)=0.01$ in figures 15–18 and for $\psi(0)=11$ for figures 19–22.
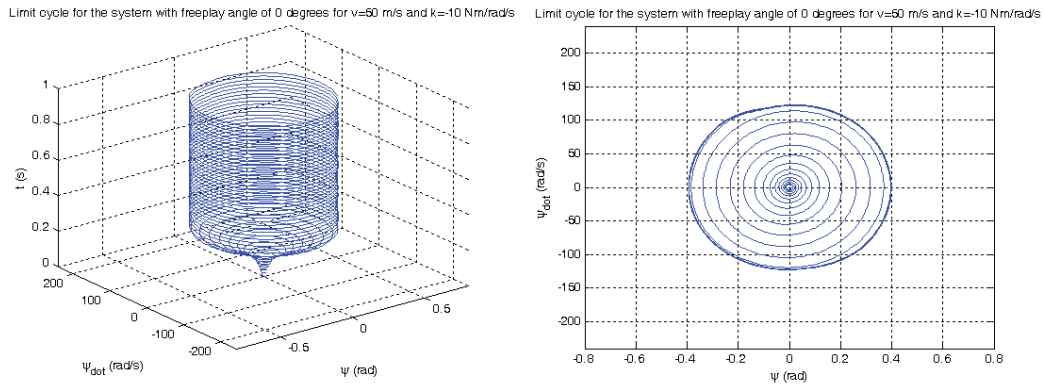

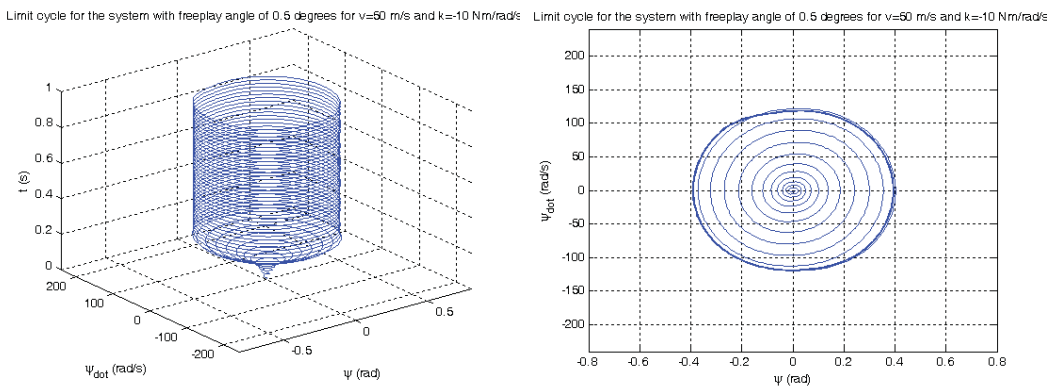*Figure 15 :* Limit cycle for ψ_{fp} of 0° and $\psi(0)=0.01$.

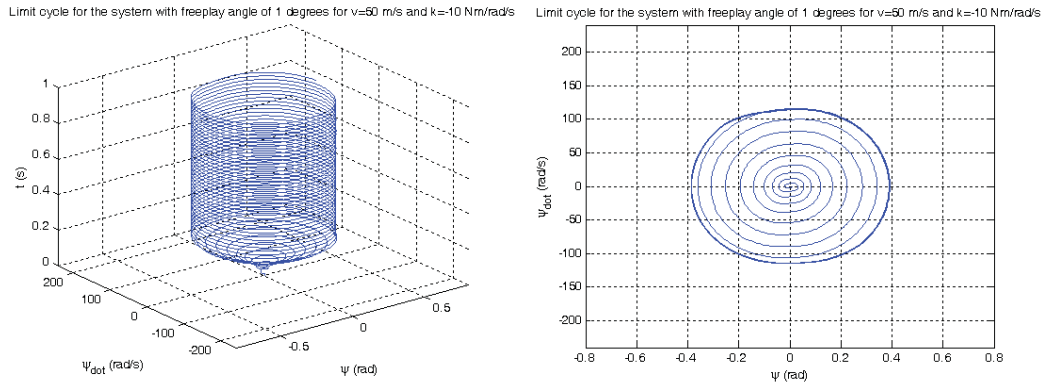*Figure 16 :* Limit cycle for ψ_{fp} of 0.5° and $\psi(0)=0.01$.

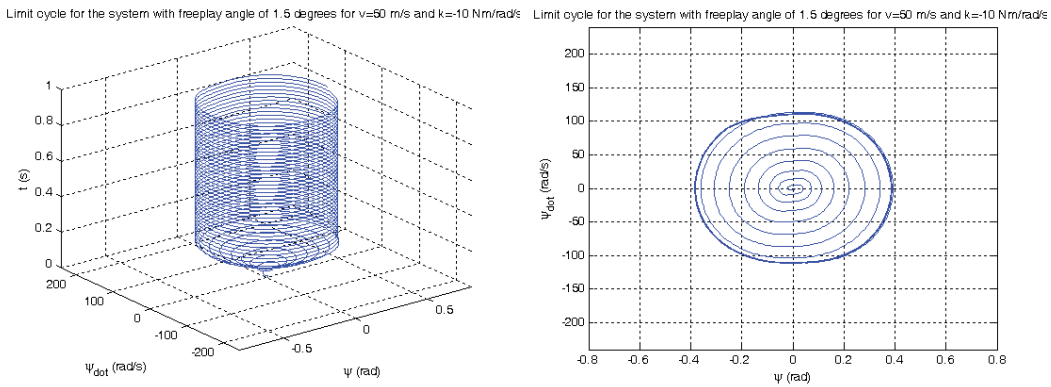Figure 17 : Limit cycle for ψ_{fp} of 1° and $\psi(0) = 0.01$.

Figure 18 : Limit cycle for ψ_{fp} of 1.5° and $\psi(0) = 0.01$.
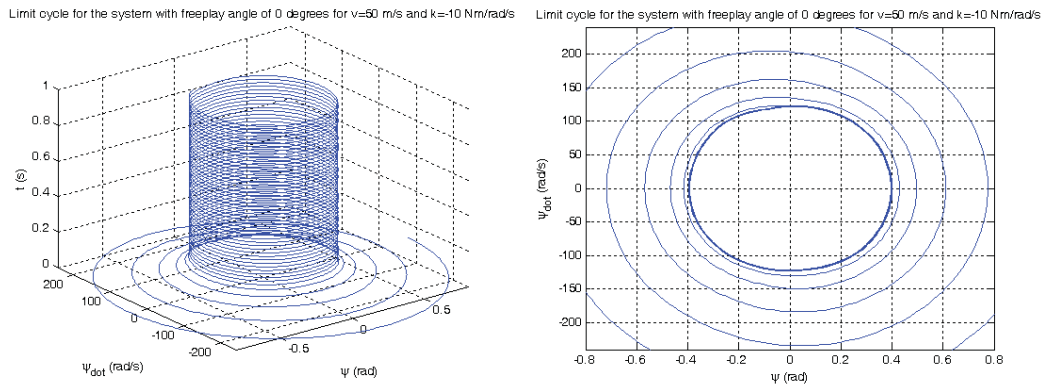

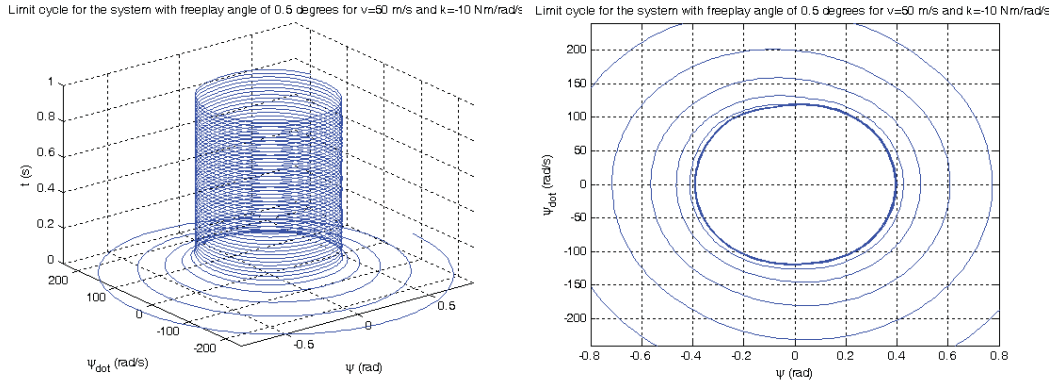Figure 19 : Limit cycle for ψ_{fp} of 0° and $\psi(0) = 1$.

Figure 20 : Limit cycle for ψ_{fp} of 0.5° and $\psi(0)=1$.
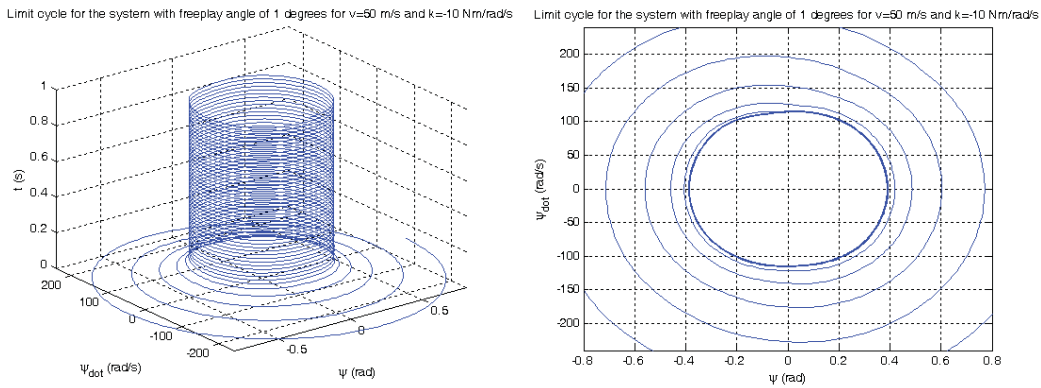

Figure 21: Limit cycle for ψ_{fp} of 1° and $\psi(0)=1$.
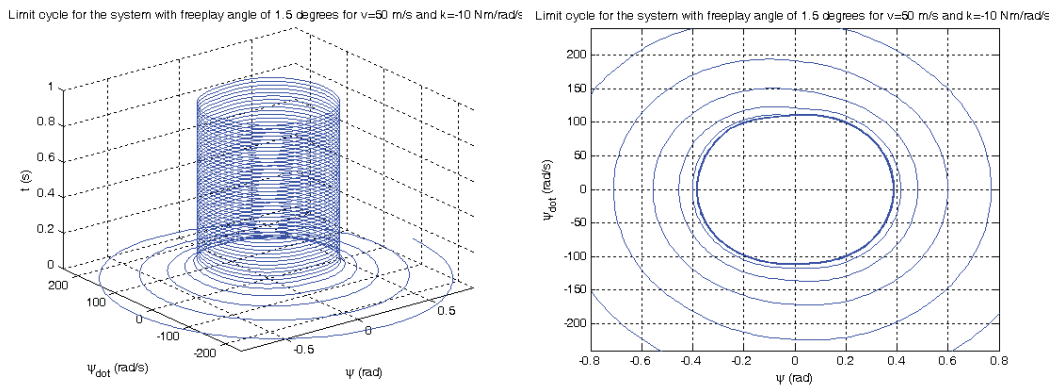

Figure 22 : Limit cycle for ψ_{fp} of 1.5° and $\psi(0)=1$.

Effect of freeplay on the torsion angle and lateral tire deformation are observed. By observing tables 2–4 it can be stated that the existence of a freeplay angle prevents shimmy damping of the system with the same physical parameters. The increase in the freeplay angle increases shimmy amplitude. A 0.5º increase of the freeplay angle from 0.5º to 1º doubles the amplitude in all 3 cases. Another 0.5º increase in the freeplay angle from 1º to 1.5º causes a 25% increase in the amplitude of the torsion angle and a 55% increase in the amplitude of the lateral tire deformation.

References Références Referencias

1. Hetreed, C., Preliminary nose landing gear shimmy analysis using MSC ADAMS Aircraft. MSC ADAMS North American User Conference.
2. Roskam, J., 2000: Airplane Design, Part IV: Layout of Landing Gear and Systems, DAR Corporation.
3. Nybakken, G. H., 1973: Investigation of Tire Parameter Variations in Wheel Shimmy, Dissertation,University of Michigan.
4. Krüger, W., Besselink, I., Cowling, D., Doan, D. B., Kortüm, W., Krabacher, W., 1997: Aircraft Landing Gear Dynamics, Simulation and Control. *Vehicle System Dynamics*, vol. 28, pp. 119–158.
5. Esmailzadeh, E., Farzaneh, K. A., 1999: Shimmy Vibration Analysis of Aircraft Landing Gears. *Journal of Vibration and Control*, vol. 5, pp. 45–56.
6. Wood, G., Blundell, M., Sharma, S., 2011: A Low Parameter Tire Model for Aircraft Ground Dynamic Simulation, Materials and Design.
7. Besselink, I. J. M., 2000: Shimmy of Aircraft Main Landing Gears, Dissertation, Technical University of Delft.
8. Maas, J. W. L. H., 2009: A Comparison of Dynamic Tire Models for Vehicle Shimmy Stability Analysis, Dissertation, Eindhoven University of Technology.
9. Esmailzadeh, E., Farzaneh, K. A., 1999: Shimmy Vibration Analysis of Aircraft Landing Gears. *Journal of Vibration and Control*, vol. 5, pp. 45–56.
10. Sura, N. K., Suryanarayan, S., 2007: Lateral response of nonlinear nose–wheel landing gear models with torsional freeplay. *Journal of Aircraft*, vol. 44, no. 6, pp. 1991–1997.
11. Long, S. H., 2006: Active Control of Shimmy Oscillation in Aircraft Landing Gear, Dissertation, Concordia University.
12. Sura, N. K., Suryanarayan, S., 2009: Lateral stability of aircraft nose–wheel landing gear with closed loop shimmy damper. *Journal of Aircraft*, vol. 46, no. 2, pp. 505–509.
13. Podgorski, W. A., 1974: The Wheel Shimmy Problem, Its Relationship to Longitudinal Tire Forces, Vehicle Motions and Normal Load Oscillations, Dissertation: Cornell University.
14. Gordon, J. T., 1977: A Perturbation Method for Predicting Amplitudes of Nonlinear Wheel Shimmy, Dissertation, University of Washington.
15. Baumann, J. A., 1992: Aircraft Landing Gear Shimmy, Dissertation, University of Missouri.
16. Stepan, G., 1991: Chaotic Motion of Wheels. *Vehicle System Dynamics*, vol. 20, no. 6, pp. 341–351.
17. Besselink, I. J. M., Schmeitz, A. J. C., Pacejka, H. B., 2010: An improved Magic Formula/Swift tire model that can handle inflation pressure changes. *Vehicle System Dynamics*, vol. 48, supplement, pp. 337–352.
18. Takacs, D., Orosz, G., Stepan, G., 2009: Delay effects in shimmy dynamics of wheels with stretched string– like tires. *European Journal of Mechanics A/Solids*, vol. 28, pp. 516–525.
19. Takacs, D., Stepan, G., 2009: Experiments on Quasiperiodic Wheel Shimmy. *Journal of Computational and Nonlinear Dynamics*, vol. 4.
20. Thota, P., Krauskopf, B., Lowenberg, M., Coetzee, E., 2010: Influence of tire inflation pressure on nose landing gear shimmy. *Journal of Aircraft*, vol. 47, no. 5, pp. 1697–1706.
21. Thota, P., Krauskopf, B., Lowenberg, M., 2009: Interaction of torsion and lateral bending in aircraft nose landing gear shimmy. *Nonlinear Dynamics*, vol. 57, pp. 455–467.
22. Plakhtienko, N. P., Shifrin, B. M., 2002: On Transverse Vibration of Aircraft Landing Gear. *Strength of Materials*, vol. 34, no. 6, pp. 584–591.
23. Plakhtienko, N. P., Shifrin, B. M., 2006: Critical Shimmy Speed of Nonswiveling Landing Gear Wheels Subject to Lateral Loading. *International Applied Mechanics*, vol. 42, no. 9, pp. 1077–1084.
24. Sura, N. K., Suryanarayan, S., 2007: Lateral response of nose–wheel landing gear system to ground induced excitation. *Journal of Aircraft*, vol. 44, no. 6, pp. 1998–2005.
25. Sura, N. K., Suryanarayan, S., 2007: Closed form analytical solution for the shimmy instability of nose wheel landing gears. *Journal of Aircraft*, vol. 44, no. 6, pp. 1985–1990.
26. Zhuravlev, V. P., Klimov, D. M., 2009: The causes of the shimmy phenomenon. *Doklady Physics*, vol. 54, no. 10, pp. 475–478.
27. Thota, P., Krauskopf, B., Lowenberg, M., 2010: Bifurcation analysis of nose landing gear shimmy with lateral and longitudinal bending. *Journal of Aircraft*, vol. 47, no.1, pp. 87–95.
28. Zhou, J. X., Zhang, L., 2005: Incremental harmonic balance method for predicting amplitudes of a multi dof nonlinear wheel shimmy system with combined Coulomb and quadratic damping. *Journal of Sound and Vibration*, vol. 279, pp. 403–416.
29. Somieski, G., 1997: Shimmy Analysis of a Simple Aircraft Nose Landing Gear Model Using Different Mathematical Methods. *Aerospace Science and Technology*, no. 8, pp. 545–555.
30. Chartier, B., Tuohy, B., Retallack, J., Tennant, S., –: Landing gear shock absorber. Research project. ftp://ftp.uniduisburg.de/FlightGear/Docs/Landing_G

ear Shock_Absorber.pdf accessed on November 23 2011

31. Dimitrijevic, Z., Mortchelewicz, G. D., Poirion, F., 2000: Nonlinear dynamics of a two dimensional airfoil with freeplay in an inviscid compressible flow. *Aerospace Science and Technology*, vol. 4, pp. 125 133.

32. Zhao, H., Cao, D., Zhu, X., 2010: Aerodynamic flutter and limit cycle analysis for a 2d wing with pitching freeplay in the supersonic flow. *3rd International Symposium on Systems and Control in Aeronautics and Astronautics*, Harbin, China, June 8–10, pp. 1105–1109.

33. Arevalo, F., Garcia–Fogeda, P., 2010: Aeroelastic characteristics of slender wing/bodies with freeplay nonlinearities. *Proceedings of the Institution of Mechanical Engineers, Journal of Aerospace Engineering*, vol. 225, pp. 347–359.

34. Marsden, C. C., Price, S. J., 2005: The aeroelastic response of a wing section with a structural freeplay nonlinearity: An experimental investigation. *Journal of Fluids and Structures*, vol. 21, pp. 257–276.

35. De–Min, Z., Qi–Chang, Z., 2010: Bifurcation and chaos analysis for aeroelastic airfoil with freeplay structural nonlinearity in pitch. *Chinese Physics B*, vol. 19, no. 3.

36. Zenthner, I., Poirion, F., 2006: Non–smooth dynamics and stability of mechanical systems featuring a freeplay nonlinearity. *International Journal of Nonlinear Mechanics*, vol. 41, pp. 796–806.

37. Kim, D., Lee, I., 2000: Transonic and low supersonic aeroelastic analysis of a two degree of freedom airfoil with a freeplay nonlinearity. *Journal of Sound and Vibration*, vol. 234, no. 5, pp. 859–880.

38. Sura, N. K., Suryanarayan, S., 2007: Lateral response of nonlinear nose–wheel landing gear models with torsional freeplay. *Journal of Aircraft*, vol. 44, no. 6, pp. 1991–1997.

39. Conner, M. D., Tang, D. M., Dowell, E. H., Virgin, L. N., 1997: Nonlinear behavior of a typical airfoil section with control surface freeplay: a numerical and experimental study. *Journal of Fluids and Structures*, vol. 11, pp. 89–109.

40. Yoo, J., Park, Y., Lee, I., Han, J., 2005: Aeroelastic analysis of a wing with freeplay in the subsonic/transonic regions. *JSME International Journal Series B*, vol. 48, no. 2, pp. 208–211.

41. Zhao, D., Zhang, Q., Tan, Y., 2009: Random flutter of a 2 dof nonlinear airfoil in pitch and plunge with freeplay in pitch. *Nonlinear Dynamics*, vol. 58, pp. 643 654.

42. Chung, K. W., Chan, C. L., Lee, B. H. K., 2007: Bifurcation analysis of a two degree of freedom aeroelastic system with freeplay structural nonlinearity by a perturbation–incremental method. *Journal of Sound and Vibration*, vol. 299, pp. 520–539.

43. Liu, L., Wong, Y. S., Lee, B. H. KK., 2002: Nonlinear aeroelastic analysis using the point transformation method, part 1: freeplay model. *Journal of Sound and Vibration*, vol. 253, no. 2, pp. 447–469.

44. Liu, L., Wong, Y. S., Lee, B. H. K., 2002: Nonlinear aeroelastic analysis using the point transformation method, part 2: hysteresis model. *Journal of Sound and Vibration*, vol. 253, no. 2, pp. 471–483.

45. Dimitriadis, G., 2008: Bifurcation analysis of aircraft with structural nonlinearity and freeplay using numerical continuation. *Journal of Aircraft*, vol. 45, no. 3, pp. 893 905.

46. Tang, D., Dowell, E. H., 2006: Flutter and limit cycle oscillations for a wing store model with freeplay. *Journal of Aircraft*, vol. 43, no. 2, pp. 487–503.

47. Tang, D., Dowell, E. H., 2006: Experimental and theoretical study of gust response for a wing–store model with freeplay. *Journal of Sound and Vibration*, vol. 295, pp. 659–684.

48. Alighanbari, H., 2002: Aeroelastic response of an airfoil–aileron combination with freeplay in aileron hinge. *Journal of Aircraft*, vol. 39, no. 4, pp.711–713.

49. Liu, L., Dowell, E. H., 2005: Harmonic Balance Approach for an Airfoil with a Freeplay Control Surface. *AIAA Journal*, vol. 43, no. 4, pp. 802–815.

50. Trickey, S. T., 2000: Global and Local Dynamics of an Aeroelastic System with a Control Surface Freeplay Nonlinearity, Dissertation, Duke University.

51. Park, Y., Yoo, J., Lee, I., 2006: Effects of angle of attack on the aeroelastic characteristics of a wing with freeplay. *Journal of Spacecraft and Rockets*, vol. 43, no. 6, pp. 1419–1422.

52. Ganguli, R., Chopra, I., Haas, D., 1998: Simulation of helicopter rotor system structural damage, blade mistracking, friction and freeplay. *Journal of Aircraft*, vol. 35, no. 4, pp. 591–597.